

G6PD functions as a metabolic checkpoint to regulate granzyme B expression in tumor-specific cytotoxic T lymphocytes

Chunwan Lu,^{1,2} Dafeng Yang,^{2,3,4} John D Klement,^{2,3,4} Yolonda L Colson,⁵ Nicholas H Oberlies,⁶ Cedric J Pearce,⁷ Aaron H Colby,^{8,9} Mark W Grinstaff,^{8,9} Han-Fei Ding,³ Huidong Shi,³ Kebin Liu ^{2,3,4}

To cite: Lu C, Yang D, Klement JD, *et al*. G6PD functions as a metabolic checkpoint to regulate granzyme B expression in tumor-specific cytotoxic T lymphocytes. *Journal for ImmunoTherapy of Cancer* 2022;**10**:e003543. doi:10.1136/jitc-2021-003543

► Additional supplemental material is published online only. To view, please visit the journal online (<http://dx.doi.org/10.1136/jitc-2021-003543>).

Accepted 06 December 2021



© Author(s) (or their employer(s)) 2022. Re-use permitted under CC BY-NC. No commercial re-use. See rights and permissions. Published by BMJ.

For numbered affiliations see end of article.

Correspondence to

Dr Chunwan Lu;
Chunwanlu@tju.edu.cn

Dr Kebin Liu; kliu@augusta.edu

ABSTRACT

Background Granzyme B is a key effector of cytotoxic T lymphocytes (CTLs), and its expression level positively correlates with the response of patients with mesothelioma to immune checkpoint inhibitor immunotherapy. Whether metabolic pathways regulate *Gzmb* expression in CTLs is incompletely understood.

Methods A tumor-specific CTL and tumor coculture model and a tumor-bearing mouse model were used to determine the role of glucose-6-phosphate dehydrogenase (G6PD) in CTL function and tumor immune evasion. A link between granzyme B expression and patient survival was analyzed in human patients with epithelioid mesothelioma.

Results Mesothelioma cells alone are sufficient to activate tumor-specific CTLs and to enhance aerobic glycolysis to induce a PD-1^{hi} Gzmb^{lo} CTL phenotype. However, inhibition of lactate dehydrogenase A, the key enzyme of the aerobic glycolysis pathway, has no significant effect on tumor-induced CTL activation. Tumor cells induce H3K9me3 deposition at the promoter of *G6pd*, the gene that encodes the rate-limiting enzyme G6PD in the pentose phosphate pathway, to downregulate *G6pd* expression in tumor-specific CTLs. G6PD activation increases acetyl-coenzyme A (CoA) production to increase H3K9ac deposition at the *Gzmb* promoter and to increase *Gzmb* expression in tumor-specific CTLs converting them from a Gzmb^{lo} to a Gzmb^{hi} phenotype, thus increasing CTL tumor lytic activity. Activation of G6PD increases Gzmb⁺ tumor-specific CTLs and suppresses tumor growth in tumor-bearing mice. Consistent with these findings, *GZMB* expression level was found to correlate with increased survival in patients with epithelioid mesothelioma.

Conclusion G6PD is a metabolic checkpoint in tumor-activated CTLs. The H3K9me3/G6PD/acetyl-CoA/H3K9ac/*Gzmb* pathway is particularly important in CTL activation and immune evasion in epithelioid mesothelioma.

BACKGROUND

Mesothelioma is an aggressive cancer arising from mesothelial cells of the pleural cavity with limited treatment options. Immune checkpoint inhibitor (ICI) immunotherapy has recently emerged as a promising therapy for human mesothelioma.^{1–2} Anti-programmed

cell death receptor 1 (PD-1)/programmed cell death ligand 1 (PD-L1) immunotherapy has shown objective responses in patients with mesothelioma.^{3,4} Anti-PD-1 ICI immunotherapy has demonstrated durable efficacy in patients with mesothelioma.^{5,6} The Food and Drug Administration has approved pembrolizumab for certain mesotheliomas. However, despite this promising progress, ICI immunotherapy is less effective in mesothelioma as compared with other cancers such as melanoma and lung cancer. Furthermore, only a small population of mesothelioma responds to ICI immunotherapy. The lack of effective response to ICI immunotherapy in mesothelioma has been linked to the small number of tumor-infiltrating lymphocytes and immunological variations in the tumor microenvironment in mesothelioma.^{7–9} In patients with mesothelioma, granzyme B expression level in tumor-infiltrating cytotoxic T lymphocytes (CTLs) positively correlates with patient response to ICI immunotherapy.^{10,11} However, how granzyme B is regulated in tumor-specific CTLs is incompletely understood.

Metabolic reprogramming to aerobic glycolysis is a key component of T-cell activation. Inhibition of aerobic glycolysis decreases T_H1 cell differentiation. Activated T cells highly express lactate dehydrogenase A (LDHA), the enzyme that converts pyruvate to lactic acid, to support aerobic glycolysis to increase interferon gamma (IFN- γ) expression.¹² Likewise, decreased aerobic glycolysis leads to a reduction in IFN- γ production and decreased T_H1 cell differentiation.^{13,14} These findings indicate that aerobic glycolysis promotes T-cell activation and differentiation and inhibition of aerobic glycolysis may cause immune suppression. However, LDHA-associated lactate from tumor cells inhibits

IFN- γ production in tumor-infiltrating T and natural killer (NK) cells and glycolytic tumors suppress T-cell cytotoxicity.¹⁵ In addition, glutamine blockade decreases glycolytic metabolism in tumor cells to maintain a highly activated and long-lived effector T-cell phenotype in tumor-bearing mice.¹⁶ These observations determine that the aerobic glycolysis impairs T-cell activation and function in the tumor microenvironment. The mechanism underlying the contrasting roles of the aerobic glycolysis in T-cell activation and effector differentiation is currently an active research area.

The pentose phosphate pathway (PPP) is a parallel metabolic pathway of aerobic glycolysis and catalyzes glucose metabolites to generate nicotinamide adenine dinucleotide phosphate (NADPH) for antioxidant response and ribose-5-phosphate for nucleic acid synthesis. The function of PPP has mainly been studied in tumor cells,^{17,18} but experimental data are beginning to emerge for PPP function in immune cells.^{17,19} In contrast to CD4⁺ T cells, which use enhanced lactate production and aerobic glycolysis to increase IFN- γ production and T_H1 cell differentiation,^{12,13} NK cells preferentially metabolize glucose through PPP and mitochondria.¹⁹ In fact, aerobic glycolysis is detrimental to NKT-cell survival and proliferation in an antibacterial immune response.¹⁹ A systemic genomic study indicates that expression of glucose-6-phosphate dehydrogenase (G6PD), the rate-limiting enzyme in PPP, is most active in lymphocytes.¹⁷ These observations suggest that PPP may play an important function in immune cells. However, the function of PPP in T-cell response to tumor, especially its function in the context of aerobic glycolysis in T cells, is incompletely understood.

In this study, we determine that aerobic glycolysis plays an indirect role in regulating tumor-specific CTL effector expression through partitioning glucose metabolic flux from PPP. Tumor cells use H3K9me3 deposition at the *G6pd* promoter to downregulate *G6pd* expression to suppress the PPP-mediated acetyl-CoA/H3K9ac/Gzmb pathway to induce a PD-1^{hi}Gzmb^{lo} dysfunctional phenotype in tumor-reactive CTLs. In patients with human mesothelioma cancer, *GZMB* expression level correlates with patient survival time. Our findings determine that G6PD functions as a metabolic checkpoint to protect CTLs from tumor-induced exhaustion.

METHODS

Mice

Female BALB/c were purchased from Jackson Laboratory (Bar Harbor, Maine, USA) or Charles River (Frederick, Maryland, USA). Studies with mice were approved by Augusta University Institutional Animal Care and Use Committee (Protocol #2008–0162).

Cell lines

Human epitheloid mesothelioma NCI-H226 and biphasic MSTO-211H cell lines were obtained from American Type Culture Collection (Manassas, Virginia, USA). Mouse

mesothelioma AB1 cell line was obtained from Sigma-Aldrich (St. Louis, Missouri, USA). Antigen-specific T cells (2/20 CTLs) were generated and maintained as previously described.²⁰ Cell lines were tested bimonthly for mycoplasma and were mycoplasma-free at the time of all experiments.

Tumor cells and tumor-specific CTL coculture system

2/20 CTLs were maintained by weekly stimulation with AH1 peptide and irradiated spleen cells as feeder cells. For polyclonal stimulation, tissue culture plates were coated by anti-CD3 (8 μ g/mL) and anti-CD28 (10 μ g/mL) antibodies. T cells were purified from BALB/c mouse spleens using mouse CD8 negative selection kit (BioLegend, San Diego, California, USA). For tumor cell–T-cell coculture, AB1 cells were mixed with 2/20 CTLs and cultured in 24-well plates.

Mouse tumor models

AB1 cells (5×10^5 /mouse) were injected subcutaneously into the right flank of BALB/c mice. Tumor-bearing mice were treated with AG1 (40 mg/kg) intraperitoneally from day 10, once every 2 days. Tumor volume was measured and calculated by the formula [(major axis \times (minor axis)²)/2]. At experimental endpoints, mice were sacrificed, tumors were harvested, a section was formaldehyde-fixed for Ki67 staining, and the remaining portion was digested in a solution consisting of collagenase (1 mg/mL, Sigma), hyaluronidase (0.1 mg/mL, Sigma), and DNase I (30 U/mL, Thermo Fisher), mechanically homogenized through a 100 μ m filter. Red cells were lysed and the cells were analyzed by flow cytometry.

AG1 synthesis

AG1 was synthesized in LeadGen Labs (Orange, Connecticut, USA) according to the published procedures with modification.²¹ The purity of the synthesized AG1 compound is 99%–100% (online supplemental figure S1).

Flow cytometry

Samples were stained with Zombie UV (BioLegend) plus specific antibodies. Antibody information is included in online supplemental table S1. For intracellular staining, cells were stained for surface markers, treated with BD Cytofix/Cytoperm Fixation/Permeabilization Solution Kit according to manufacturer's instructions (BD Biosciences, San Diego, California, USA), and then stained for intracellular proteins. Cells were analyzed in a FACSCalibur or a LSRFortessa flow cytometer (BD Biosciences). All flow cytometry data analyses were conducted with FlowJo (BD Biosciences).

Patient dataset analysis

The Cancer Genome Atlas Program (TCGA) RNA sequencing data from the MESO cohort was accessed through Xena Browser. Fraction of CD8⁺ T cells was inputted from bulk RNA-sequencing data using

CIBERSORT. Survival analysis was performed using the R survival and survminer packages.

Immunohistochemistry

Tumor tissue was fixed in 10% formalin overnight. The fixed tissues were processed into paraffin blocks for Ki67 IHC staining.

Acetyl-coenzyme A assay

AB1 were cocultured with 2/20 CTLs in the presence of AG1 for 24 hours. 2/20 CTLs were isolated by CD45 positive selection nanobeads (BioLegend). The isolated 2/20 CTLs were measured for acetyl-CoA level using acetyl-CoA assay kit according to manufacturer instruction (Sigma-Aldrich).

Lactate assay

Tumor cocultured CTLs, AH1-stimulated CTLs and anti-CD3/28-stimulated CD8⁺ T cells were isolated by using mouse CD8 positive selection nanobeads (BioLegend). The isolated T cells were measured for lactate using the lactate assay II kit (Cat#MAK065) according to the manufacturer's instructions (Sigma-Aldrich).

Chromatin immunoprecipitation (CHIP)

ChIP was performed as previously described²² using anti-H3K9me3 (Abcam, Cambridge, Massachusetts, USA), or anti-H3K9ac (Cell Signaling Transduction) antibodies and the ChIP Assay Kit (Cell Signaling Transduction) according to the manufacturer's instructions.

Statistical analysis

Statistical analysis was done using GraphPad Prism and p values were calculated by a two-tailed Student t-test. Significance between survival groups was computed by two-sided log-rank test (Survival package, R) with p<0.05 considered as significant.

RESULTS

Tumor cell is sufficient to activate tumor-specific CTLs and to enhance aerobic glycolysis in the activated tumor-specific CTLs

Analysis of human mesothelioma cell lines revealed that human mesothelioma tumor cells express high levels of PD-L1 (online supplemental figure S2). PD-L1 expression is further increased by both type I and type II interferons in human mesothelioma cells (online supplemental figure S2). These constitutive and interferon-enhanced PD-L1 expression profiles of human mesothelioma cells indicate that human mesothelioma is potentially a type of highly immune suppressive human cancer. To model human mesothelioma immune suppression, we made use of murine mesothelioma cell line AB1. AB1 cells also express high levels of PD-L1 that is further increased by both type I and type II interferons (figure 1A), thereby resembling human mesothelioma. AB1 cells express the viral gp70 protein with the immunogenic AH1 peptide sequence (SPSYVYHGF).²³ 2/20 CTL is an antigen-specific CTL

line that recognizes the H2-L^d-restricted AH1 epitope (SPSYVYHGF/gp70₄₂₃₋₄₃₁) of gp70 protein endogenously expressed by AB1 cells.²⁰⁻²⁴ 2/20 CTLs express high level of PD-1 when activated by the AH1 peptide and can be detected by an AH1-specific tetramer (figure 1B). 2/20 CTLs kill AB1 tumor cells in a dose-dependent manner in vitro (figure 1C,D). Human mesothelioma cells primarily metastasize to the lung. AB1 cells form tumor nodules in the lung in syngeneic mice in a dose-dependent manner in an experimental lung metastasis mouse model (figure 1E). Furthermore, 2/20 CTL adoptive transfer immunotherapy suppressed AB1 tumor growth in a CTL dose-dependent manner (figure 1F).

The aforementioned findings determine that this AB1-2/20 CTL model is a defined tumor-specific CTL model for analysis of tumor cell-CTL interaction at the effector phase. It is known that aerobic glycolysis increases in activated T cells.²⁵ To determine whether tumor cells regulate aerobic glycolysis during T-cell activation, we stimulated 2/20 CTLs with anti-CD3 and anti-CD28, antigen (AH1 peptide), and AB1 tumor cells. The rationale is that anti-CD3 plus anti-CD28, as well as the antigen, should both activate the 2/20 CTLs and induce the production of lactate, a key product of aerobic glycolysis. AB1 tumor cell should also activate 2/20 CTLs through its endogenously expressed AH1 peptide. Any difference in lactate production between these activation conditions is thus due to tumor cells. Analysis of lactate in CTLs revealed that AB1 tumor cells induce a significantly higher level of lactate production compared with anti-CD3 plus anti-CD28 and AH1 peptide stimulation (figure 1G). Because there are only tumor cells and the tumor-specific CTLs in the tumor-CTL coculture system, we conclude that mesothelioma tumor cell alone is sufficient to activate the tumor-specific 2/20 CTLs and to enhance aerobic glycolysis in the activated CTLs.

Tumor-enhanced aerobic glycolysis is associated with CTL exhaustion

Aerobic glycolysis has been shown to be essential for T-cell activation and effector differentiation.¹²⁻¹³ However, the LDHA-lactate pathway has also been shown to inhibit T cells and NK-cell activation.¹⁵ The role of aerobic glycolysis in T-cell activation and function is therefore cellular context-dependent. Our aforementioned findings indicate that mesothelioma cells enhance aerobic glycolysis in tumor-specific CTLs. To determine how increased lactate regulates CTL activation, we compared phenotypes of 2/20 CTLs activated by tumor cells and the AH1 peptide antigen. PD-1 expression is an indicator of T-cell response to T-cell activation-based immunotherapy in mesothelioma.²⁶ As expected, AB1 tumor cells induced a significantly higher level of PD-1 expression on 2/20 CTLs compared with AH1 peptide antigen-activated 2/20 CTLs (figure 2A). Antigen-activated 2/20 CTLs exhibited a high expression level of *Gzmb*, a key cytotoxic effector of CTLs.¹¹ *Gzmb* expression level is significantly decreased in 2/20 CTLs cocultured with AB1 tumor cells (figure 2A).

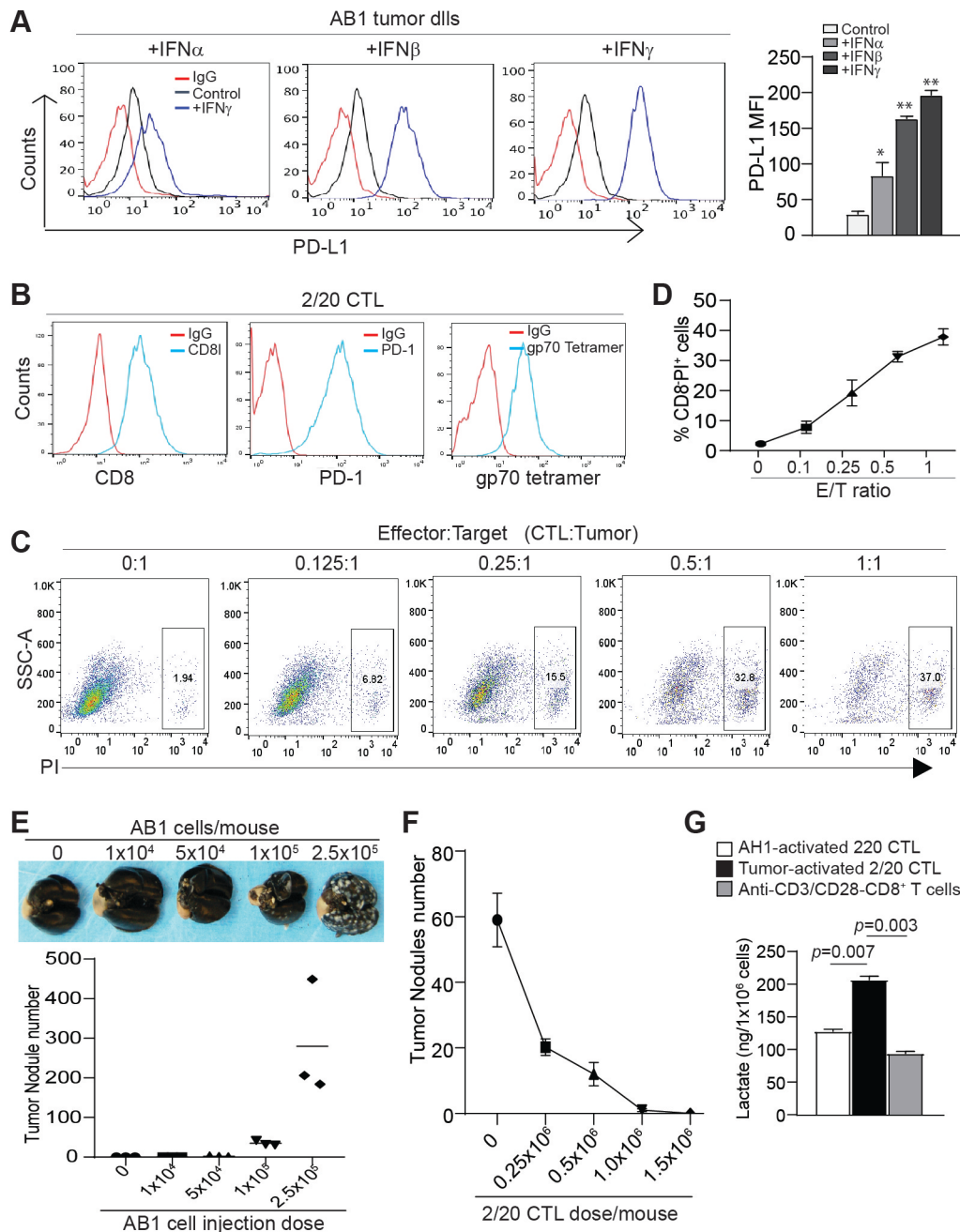


Figure 1 Tumor-specific CTL activation and function assay model. (A) AB1 tumor cells were treated by mIFN- α , mIFN- β , and mIFN- γ overnight and analyzed for PD-L1 expression by flow cytometry. The MFI of PD-L1 were quantified and presented at the right. (B) 2/20 CTLs were activated with AH1 peptides and analyzed by flow cytometry for CD8, PD-1, and gp70 expressions. (C) 2/20 CTLs were cocultured with AB1 cells for different ratios. Cell mixture were stained with CD8 and PI and analyzed by flow cytometry. (D) The percentage of CD8⁺PI⁺ dead cells were quantified and presented. (E) AB1 cells were intravenously injected into BALB/c mice tail veins at indicated doses. After 14 days, the mice were sacrificed and the lungs were inflated by India ink. Top panel shows images of representative tumor-bearing lungs. The tumor nodules were quantified and presented at the bottom. (F) AB1 cells were intravenously injected into BALB/c mice. At day 5, 2/20 CTLs were intravenously injected into the tumor-bearing mice at the indicated doses. Mice were sacrificed 14 days after tumor cell injection and the lungs were inflated by India ink. The tumor nodules were quantified. (G) 2/20 CTLs were stimulated with AH1 peptide and live AB1 tumor cells for 24 hours. CD8⁺ T cells were purified from mouse spleens and stimulated with anti-CD3/CD28 antibodies for 24 hours. Lactate concentrations were determined in these cells. * $p < 0.05$; ** $p < 0.01$. CTL, cytotoxic T lymphocyte; E:T, effector:target; IFN, interferon; MFI, mean fluorescent intensity; SSC-A, side scatter-area.

CTLs cocultured with AB1 tumor cells have a significantly lower population of PD1⁺Gzmb^{hi} cells (figure 2B). As a positive control, anti-CD3/CD28-activated primary CD8⁺

T cells express high levels of Gzmb (figure 2C). Taken together, our findings indicate that mesothelioma tumor cells not only enhance aerobic glycolysis in tumor-specific

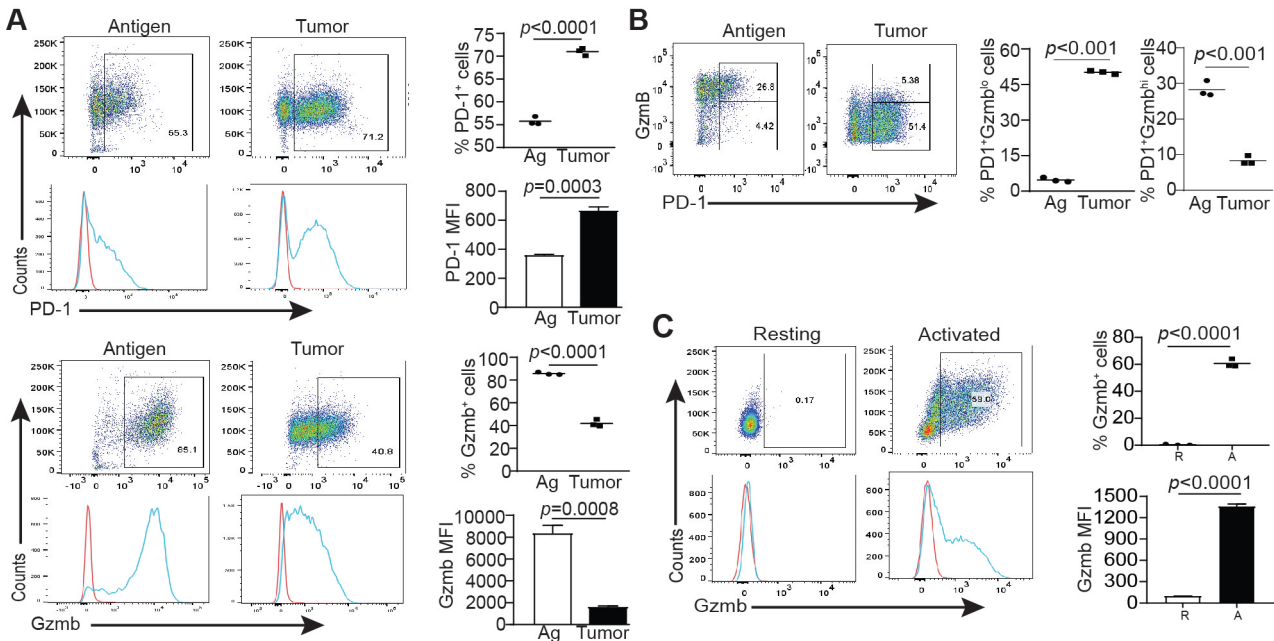


Figure 2 Tumor cells induce CTL dysfunction. (A) 2/20 CTLs were stimulated with the AH1 peptide or live AB1 tumor cells for 24 hours. Cells were stained for CD8, PD-1, and Gzmb, and analyzed by flow cytometry. Shown are representative plots and histograms at the left. The % PD-1⁺ and Gzmb⁺ cells, and PD-1 and Gzmb MFI were quantified and presented at the right. (B) Cells as shown in A were analyzed for Gzmb^{hi} and Gzmb^{lo} population in the PD-1⁺ cells as indicated under the two activation conditions. (C) Primary CD8⁺ T cells were purified from mouse spleens and activated with anti-CD3/CD28 antibodies for 24 hours. Resting (R) and activated (A) CD8⁺ T cells were stained for CD8 and Gzmb, and analyzed by flow cytometry. Shown are plots of percentage of positive cells and histograms for Gzmb in CD8⁺ T cells. The quantifications are shown at the right panel.

CTLs but also induce tumor-specific CTL dysfunction with a PD-1^{hi}Gzmb^{lo} phenotype.

Tumor-enhanced aerobic glycolysis is not directly linked to tumor-specific CTL exhaustion

The aforementioned findings suggest that mesothelioma cells may use enhanced aerobic glycolysis to induce tumor-specific CTL exhaustion. To test this hypothesis, we cocultured AB1 tumor cells with 2/20 CTLs in the presence of an inhibitor of LDHA, the rate-limiting enzyme that converts pyruvate to lactic acid. The tumor-activated CTLs were then gated from the tumor cell-CTL population and analyzed for cell surface markers. Inhibition of LDHA decreased CTL numbers, although at a small level (online supplemental figure S3). Surprisingly, inhibition of LDHA showed no significant effect on the levels of PD-1⁺ and Gzmb⁺ tumor-specific CTLs (online supplemental figure S3). This finding indicates that aerobic glycolysis plays no direct role in mesothelioma cell induction of tumor-specific CTL exhaustion.

G6PD functions as a metabolic checkpoint to control glucose metabolic flux partitioning and tumor-induced CTL exhaustion

T-cell function can be regulated by a divergent metabolic program.¹⁶ PPP is a parallel pathway of glycolysis. We therefore hypothesized that PPP promotes CTL activation and tumor cells may use enhanced aerobic glycolysis to diverge glucose metabolic flux away from PPP to induce CTL exhaustion. G6PD is the rate-limiting enzyme of PPP.

T-cell exhaustion is known to be regulated by exhaustion-specific epigenetic enhancers.²⁷ Epigenetic dysregulation, particularly alterations of H3K9 methylation-mediated gene expression, is a major mechanism underlying dysregulation of metabolic pathways and T-cell activation in the tumor microenvironment.^{28–30} We therefore analyzed H3K9me3 deposition at the *G6pd* promoter. ChIP analysis determined H3K9me3 deposition at the *G6pd* promoter in tumor-specific 2/20 CTLs (figure 3A,B). Treatment of the coculture mixture of AB1 tumor cell and 2/20 CTLs with a H3K9me3 histone methyltransferase-selective inhibitor verticillin A³¹ decreased H3K9me3 deposition at the *G6pd* promoter (figure 3B). Consistent with the decreased H3K9me3 deposition, verticillin A treatment significantly increased *G6pd* expression in the tumor-specific CTLs (figure 3C).

G6PD is the rate-limiting enzyme in PPP, the parallel metabolic pathway of aerobic glycolysis. Our aforementioned findings that tumor cells simultaneously enhance aerobic glycolysis and induce G6PD downregulation suggest that tumor cells may use inducing G6PD downregulation to suppress PPP as a mechanism to partition glucose metabolic flux to aerobic glycolysis to induce tumor-specific CTL exhaustion. PPP suppression, not aerobic glycolysis increase, may thus underlie tumor-activated CTL exhaustion. If this is the case, activating G6PD then should reactivate PPP to reverse tumor cell-induced CTL exhaustion. We therefore made use of the

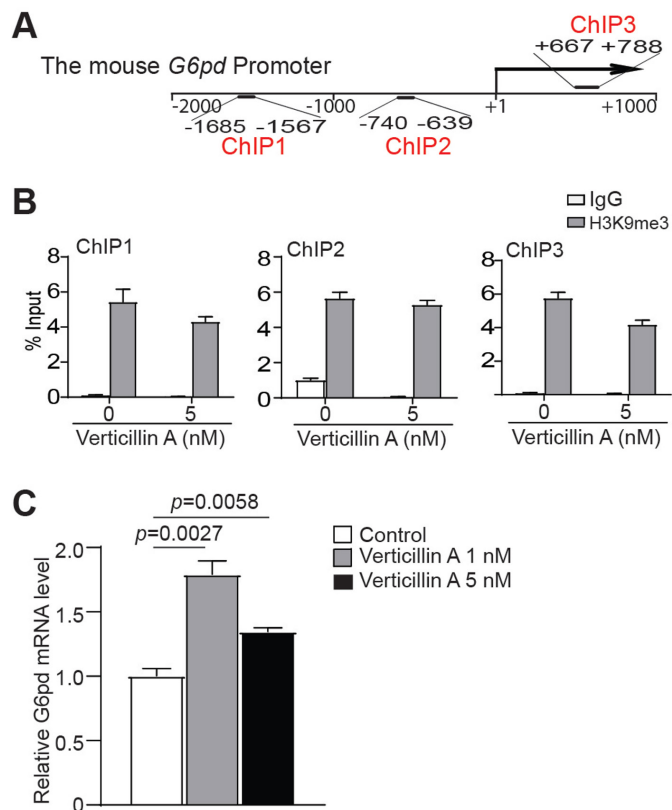


Figure 3 Inhibition of H3K9me3 activates *G6pd* expression in tumor-specific CTLs. (A) The mouse *G6pd* promoter structure showing ChIP sites. (B) 2/20 CTLs were cocultured with live AB1 tumor cells in the presence of verticillin A and analyzed by ChIP using IgG or H3K9me3-specific antibody. (C) 2/20 CTLs were cocultured with live AB1 tumor cells in the presence of verticillin A for 24 hours. 2/20 CTLs were isolated and analyzed by qPCR for *G6PD* mRNA level. ChIP, chromatin immunoprecipitation; CTL, cytotoxic T lymphocyte.

recently developed G6PD activator AG1.²¹ 2/20 CTLs were cocultured with AB1 tumor cells in the presence of AG1. Cell mixture was stained with CD8⁺ and *Gzmb*-specific mAb. Live CD8⁺ cells were gated and analyzed for *Gzmb* expression (figure 4A). AG1 treatment increased *Gzmb*⁺ CTLs in a dose-dependent manner in vitro (figure 4B). However, AG1 treatment decreased *Gzmb* expression in both antigen-activated 2/20 CTLs (online supplemental figure S4A,B) and anti-CD3/CD28-activated primary CD8⁺ T cells in vitro (online supplemental figure S4C,D).

To determine whether this finding can be extended to CTL activation in the tumor microenvironment in vivo, we established AB1 tumors in syngeneic mice and allowed the tumors to grow to a large size so that AG1 treatment did not significantly decrease tumor size and unmask tumor burden on immune cell infiltration (figure 4C). The tumor-bearing mice were then treated with AG1. Although the total CD45⁺ tumor-infiltrating leukocyte level is not changed, AG1 treatment significantly decreased total tumor-infiltrating CD8⁺ T cells and the tumor antigen (gp70)-specific CTLs (figure 4D,E). However, AG1 significantly increased the activated tumor-specific CTLs (*Gzmb*⁺gp70 tetramer⁺ CD8⁺) in the tumor

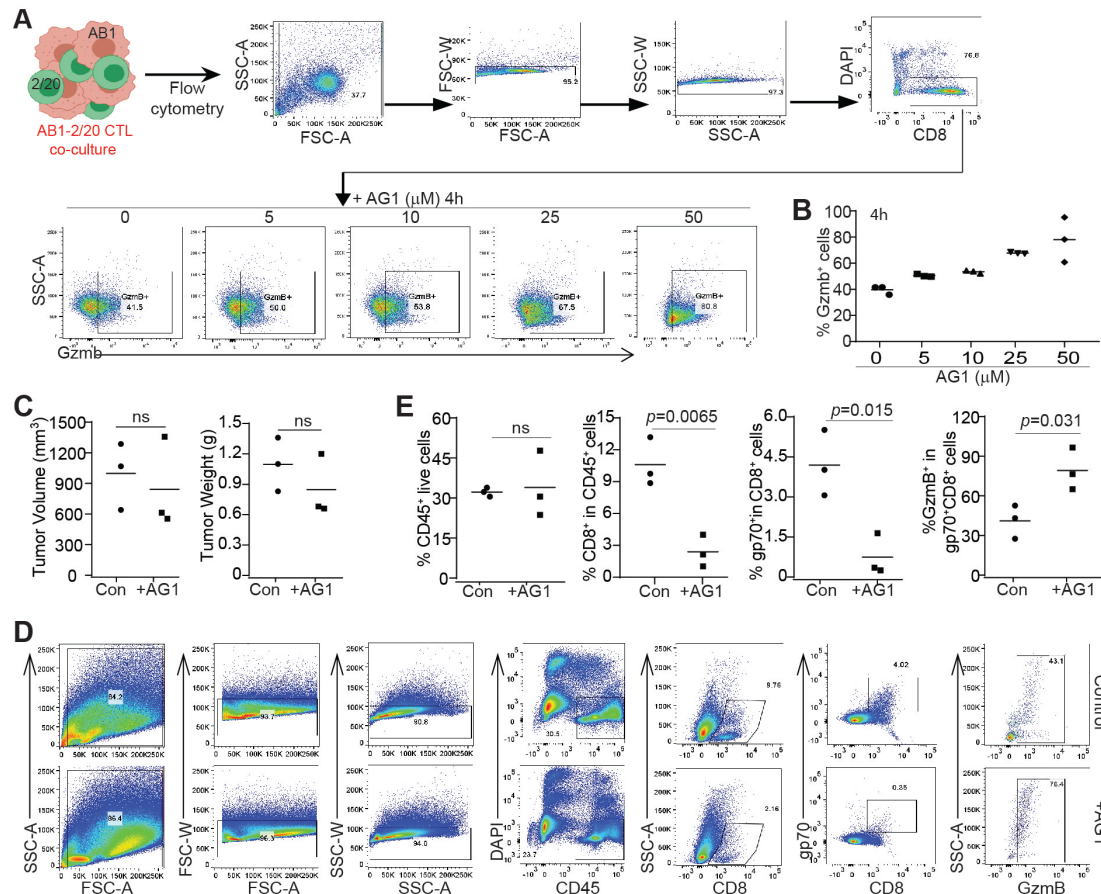
microenvironment (figure 4D,E). Taken together, our data indicate that the G6PD-PPP metabolic pathway enhances tumor-specific CTL activation in vivo.

G6PD regulates acetyl-CoA production and the *Gzmb* promoter H3K9 acetylation to upregulate *Gzmb* expression in tumor-reactive CTLs

H3K9 acetylation is a chromatin modification associated with gene transcription activation.³² H3K9ac has been shown to regulate activation of T cell effectors such as IFN- γ .¹² The mitochondrial acetyl-CoA is an essential substrate for histone acetylation. Recent study showed that *G6PD* is essential for mitochondrial function³³ and mitochondrial metabolic pathway regulates *Gzmb* expression in T cells.³⁴ It is known that the PPP metabolic pathway enhances mitochondrial acetyl-CoA production.³⁵ Analysis of genome-wide H3K9ac ChIP-Seq dataset in human T cells identified H3K9ac deposition at the *GZMB* promoter (figure 5A). We therefore hypothesized that activation of the G6PD enhances acetyl-CoA production to increase H3K9ac deposition at the *Gzmb* promoter to activate *Gzmb* expression in tumor-specific CTLs. To test this hypothesis, 2/20 CTLs were cocultured with AB1 tumor cells in the presence of AG1. 2/20 CTLs were then isolated from the coculture mixture, and the acetyl-CoA concentration was measured. AG1 treatment increased acetyl-CoA level in 2/20 CTLs in a dose-dependent manner (figure 5B). To determine whether increased acetyl-CoA leads to increased H3K9ac deposition at the *Gzmb* promoter in tumor-specific CTLs, we then cocultured 2/20 CTLs with AB1 tumor cells and treated the cocultures with AG1. Analysis of the CTLs detected H3K9ac deposition at the *Gzmb* promoter region in 2/20 CTLs. Furthermore, AG1 treatment increased H3K9ac deposition at a region around the *Gzmb* transcription start site in 2/20 CTLs (figure 5C). These observations indicate that the G6PD-PPP metabolic pathway regulates acetyl-CoA production and H3K9ac deposition at the *Gzmb* promoter to activate *Gzmb* expression in tumor-specific CTLs.

Pharmacological activation of G6PD increases CTL tumor lytic activity in vitro and suppresses tumor growth in vivo

To determine whether the above finding that G6PD activation increases *Gzmb*⁺ tumor-specific CTLs can be translated to increased CTL effector function, we assessed in vitro CTL killing efficacy in this defined 2/20 CTL and AB1 tumor cell co-culture system. To unmask the direct tumor cell cytotoxicity of AG1 from its function in enhancing CTL lytic function, we first analyzed AG1 cytotoxicity to tumor cells by mixing AB1 tumor cells with purified spleen primary CD8⁺ T cells. The spleen primary CD8⁺ T cells were used as a negative control for the 2/20 CTLs. The cell mixture was treated with AG1 and analyzed for tumor cell death. AG1 showed direct cytotoxicity against AB1 tumor cells (figure 6A). 2/20 CTLs and AB1 tumor cells were then cocultured in the presence of various concentrations of AG1. The culture mixture was stained with CD8 and PI (Propidium Iodide) and gated into CD8⁺ tumor



cells and CD8⁺ CTLs. Cell death was measured in both the CD8⁻ tumor cells and CD8⁺ CTLs, and normalized based on live CTLs at the given AG1 concentrations (figure 6B). AG1 increased 2/20 CTL-mediated AB1 tumor cell lysis (figure 6C). Although AG1 induces CTL cell death (figure 6B), AG1 did not significantly alter proliferation of the live CTLs (online supplemental figure S5).

To determine whether this finding can be translated to tumor growth suppression in vivo, AB1 cells were subcutaneously injected into immune competent mice. The tumor-bearing mice were then treated with AG1. AG1 exhibited a significant efficacy in suppression of tumor growth (figure 6D). Consistent with tumor growth inhibition, AG1 therapy significantly decreased tumor cell proliferation in vivo (figure 6E,F). Taken together, our data indicate that G6PD acts as a tumor suppressor and does so at least in part through enhancing tumor-reactive CTL lytic activity.

GZMB level correlates with increased survival in patients with epithelioid mesothelioma

To determine the human relevance, we performed analysis of the human mesothelioma bulk mRNA expression

datasets in TCGA database. AB1 is an epithelioid-like murine mesothelioma cell line.³⁶ The available human epithelioid mesothelioma specimens (n=58) were analyzed. CD8 and *GZMB* expression levels of the epithelioid tumor specimens were plotted for patient survival time. CTL tumor infiltration level is not correlated with overall survival in patients with human epithelioid mesothelioma (figure 7A). Instead, higher *GZMB* expression level is significantly correlated with increased overall survival in patients with human epithelioid mesothelioma (figure 7B). Taken together, our observations indicate that tumor-infiltrating CTL effector granzyme B expression level and function, not CTL infiltration level, determine tumor growth control and patient survival in human patients with epithelioid mesothelioma.

DISCUSSION

An important consequence of aerobic glycolysis in the tumor microenvironment is the creation of a hypoxic, acidic, nutrient-depleted tumor microenvironment

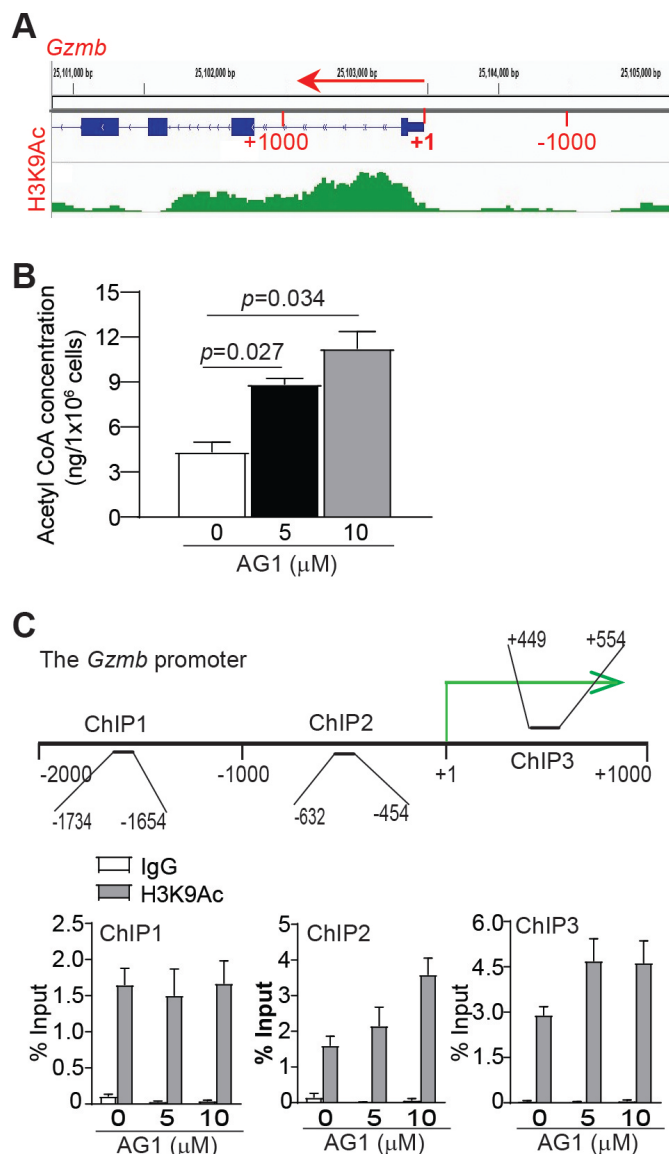


Figure 5 G6PD increases acetyl-CoA generation and H3K9ac deposition at the *Gzmb* promoter in tumor-specific CTLs. (A) H3K9ac ChIP-Seq dataset in human T cells was extracted from GEO database. H3K9ac deposition level at the *GZMB* promoter is shown. (B) 2/20 CTLs were co-cultured with AB1 tumor cells in the presence of AG1 at the indicated concentrations for 24 hours. The T cells were isolated and analyzed for acetyl-CoA concentration. (C) The *Gzmb* promoter with ChIP locations is shown at the top panel. Bottom panel: 2/20 CTLs were cocultured with AB1 tumor cells and treated with AG1 as in B, followed by ChIP using H3K9ac-specific antibody. ChIP, chromatin immunoprecipitation; CTL, cytotoxic T lymphocyte.

that is hostile to antitumor immune responses.¹⁶ The specialized metabolic programming of tumor cells not only directly promotes tumor growth but also engages T cells to impair an effective antitumor immune response, likely by inducing T-cell exhaustion.^{37,38} However, aerobic glycolysis has been shown to play contrasting roles and can either enhance^{12,39} or suppress¹⁵ T-cell activation and effector function. Using a defined tumor cell and tumor cell-specific

CTL coculture system, we determined that tumor cells enhance lactate production in tumor-specific CTLs, thereby validating the findings that tumor cells promote aerobic glycolysis in tumor-specific CTLs.¹⁵ However, we observed that inhibition of LDHA, the key enzyme in the aerobic glycolysis pathway that converts pyruvate to lactate, failed to reverse tumor-induced CTL exhaustion. Targeting LDHA has shown mixed results in tumor cells and T cells.¹² Our findings suggest that aerobic glycolysis plays an indirect role in mesothelioma cell induction of tumor-specific CTL exhaustion.

PPP is a parallel metabolic pathway to glycolysis that also metabolize glucose. Aerobic glycolysis and PPP therefore may compete for the glucose metabolic flux. In this study we determined that *G6pd* is downregulated by its promoter H3K9me3 deposition in tumor-activated CTLs. Furthermore, we determined that activation of G6PD reverses tumor-induced CTL exhaustion. G6PD is the rate-limiting enzyme of PPP. Our findings thus suggest that tumor cells may use inducing H3K9me3 deposition to repress *G6pd* expression to decrease PPP metabolic flux to divert glucose metabolic flux to aerobic glycolysis, resulting in tumor-activated CTL exhaustion. G6PD may thus act as a 'metabolic checkpoint' that controls glucose metabolic flux partitioning between aerobic glycolysis and PPP. Consistent with this notion, we determined that pharmacological activation of G6PD enhances the acetyl-CoA/H3K9ac pathway to reverse CTL exhaustion to increase PD-1^{lo}*Gzmb*⁺ CTL subset to enhance CTL lytic function in tumor cell lysis in vitro and tumor growth suppression in vivo. G6PD is therefore potentially a molecular target for metabolic reprogramming of tumor-specific CTLs to reverse immune suppression in cancer immunotherapy.

One challenge in translating G6PD activation to human cancer immunotherapy is that G6PD activation decreases total tumor-infiltration CTL level in vivo. A recent genomic synthetic lethal study revealed that *G6pd* is the most dominant gene in mammalian cells in mitochondrial oxidative function.³³ In this study, we determined that G6PD activation increases CTL activation. It is known that T-cell turnover is regulated by activation-induced cell death.⁴⁰ It is therefore possible that G6PD activation enhances CTL activation, resulting in increased activation-induced cell death to decrease total CTL level in the tumor microenvironment. The relationship between G6PD and activation-induced CTL death in the tumor microenvironment thus requires further study.

Although the total CTL level decreased, the activated tumor-specific (gp70⁺*Gzmb*⁺) CTLs are apparently increased significantly by AG1 therapy in tumor-bearing mice. It is known that antigen-specific effector CTLs are protected from apoptosis during an active immune response.⁴¹ It is also known that only subsets of CTLs, not all tumor-infiltrating CTLs, are responsible for tumor lysis.^{42,43} In addition, T-cell response to tumor cells depends on metabolic programs that are specific to T-cell subsets.¹⁶ Therefore, although AG1 may decrease

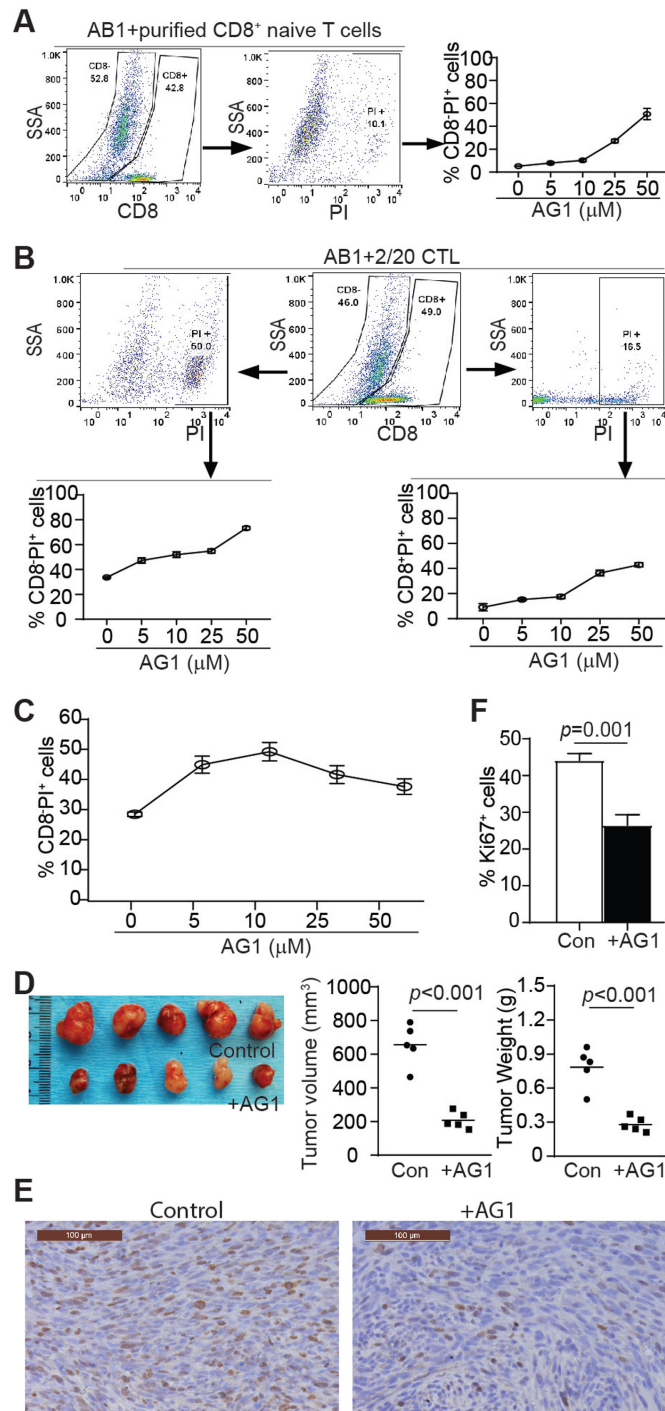


Figure 6 G6PD increases CTL lytic function in vitro and suppress tumor growth in vivo. (A) AB1 cells were cultured with purified primary CD8⁺ T cells in the presence of AG1 at the indicated concentrations for 24 hours. The cell mixtures were stained for CD8 and PI and analyzed by flow cytometry. CD8⁻ tumor cells were quantified for cell death. (B) AB1 cells were cultured with the tumor-specific 2/20 CTLs in the presence of AG1 at the indicated concentrations. Tumor cells and CTL death were analyzed by PI staining and flow cytometry. (C) 2/20 CTL-specific killing of tumor cells were normalized by minus AG1-induced tumor cell death as in A and normalized by live 2/20 CTLs percentage. (D) AB1 cells were injected subcutaneously in BALB/c mice. Ten mice with similar tumor size were randomly placed into two groups and treated with solvent or AG1 (40 mg/kg) daily for nine times. The tumor image is shown at the left panel; tumor size and weight were quantified and presented at the right panel. (E) The tumor tissues as shown in D were analyzed by immunohistochemical staining with Ki67-specific antibody. (F) The percentage of Ki-67-positive cells as shown in E was quantified. CTL, cytotoxic T lymphocyte.

total tumor-infiltrating CTL level, the activated tumor-specific CTLs are increased in the tumor microenvironment after AG1 therapy. Our findings suggest that tumor-specific tumor-infiltrating CTLs, not the total tumor-infiltrating CTL level,

contribute to mesothelioma suppression in tumor-bearing mice.

It appears that total CTL tumor-infiltrating level, although critically important in many types of human

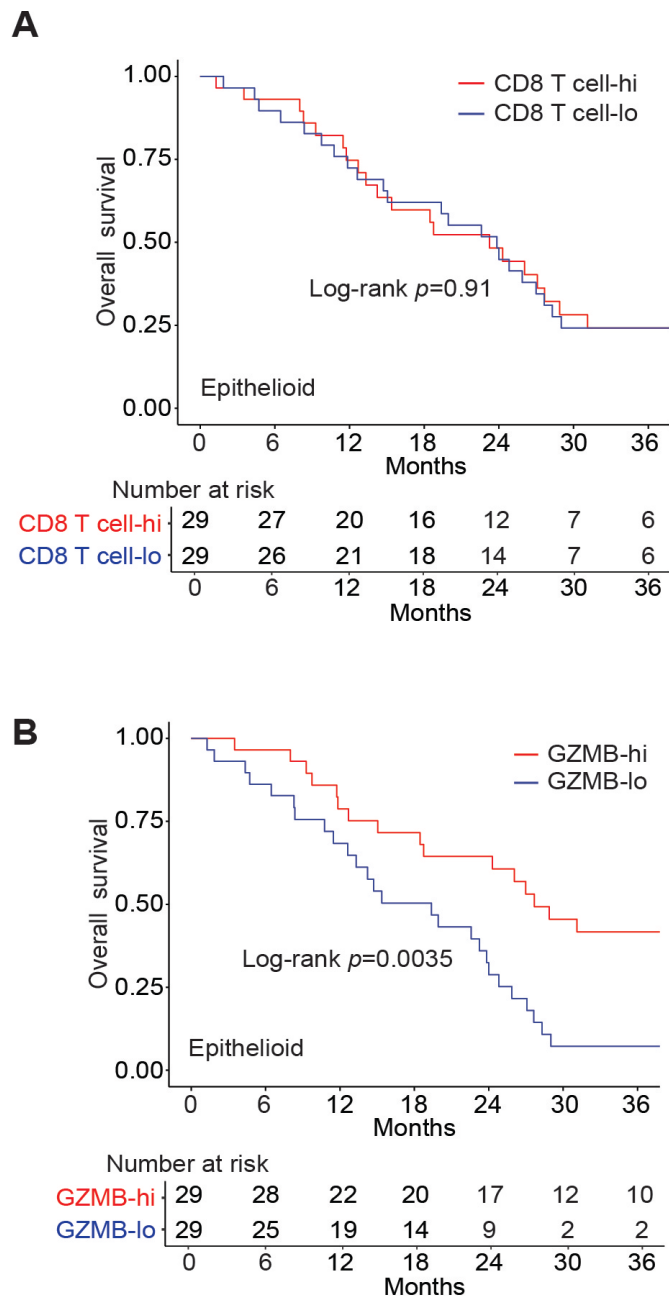


Figure 7 Granzyme B expression level correlates with patient survival time. (A) CD8 datasets of patients with human epithelioid mesothelioma were extracted from TCGA database and plotted for patient survival. (B) *Gzmb* mRNA datasets of human epithelioid mesothelioma were extracted from TCGA database and plotted for patient survival.

cancers, may not be a determining factor in epithelioid mesothelioma tumor growth control as determined by patient survival. One recent study revealed that CD3⁺, CD4⁺ and CD8⁺ T cell tumor-infiltrating density is correlated with significantly worse clinical outcomes in patients with mesothelioma.⁴⁴ Additional studies have also shown that CD8⁺ T-cell tumor-infiltrating density is correlated with significantly worse clinical outcomes in patients with mesothelioma,^{45 46} with one of the studies also noting that tumor-infiltration density of CD4⁺ T

cells is correlated with longer survival, and thus a lower CD4:CD8 ratio achieves worse survival.^{46–48} In this study, we made use of the bulk RNA-Seq dataset and observed that CD8 T-cell level is not correlated with the survival of patients with epithelioid mesothelioma. While characterizing cell subsets based on genomic datasets in high tumor-infiltrating lymphocytes have been widely used, data generated from this approach for tissues such as malignant pleural mesothelioma with in-tumor variations and low T-cell numbers may have only limited implications.⁴⁹ In addition, our tumor-bearing mouse studies determined that tumor-specific CD8⁺ T cells and CTL functional status, not the total CD8⁺ T cells, contribute to mesothelioma suppression in epithelioid mesothelioma tumor-bearing mice. Our findings suggest that CTL functionality, not CTL level, is the determining factor in host immune surveillance in human epithelioid mesothelioma. This notion is further supported by the observations that granzyme B-expressing CTL level increase is correlated with better clinical outcomes in patients treated with immune checkpoint blockade immunotherapy in patients with human mesothelioma and lung cancer.^{10 11 50} Therefore, despite decreased total CTL level in the tumor microenvironment, AG1 targeted therapy selectively increased tumor-specific and activated CTLs in the tumor, resulting in tumor suppression. Pharmacological activation of G6PD is therefore potentially a selective CTL function-based approach for human epithelioid mesothelioma immunotherapy.

CONCLUSION

The role of aerobic glycolysis in T-cell activation and exhaustion has been well established. PPP is a parallel metabolic pathway of glycolysis that may compete for glucose metabolic flux with glycolysis. G6PD is the rate-limiting enzyme in PPP. In this study, we demonstrated that the tumor cell alone is sufficient to enhance aerobic glycolysis in tumor-specific CTLs and to induce a PD-1^{hi}Gzmb^{lo} exhaustion phenotype. Surprisingly, increased aerobic glycolysis is not directly linked to tumor-specific CTL exhaustion since inhibition of LDHA has no significant effect on the tumor-specific CTL exhaustion phenotype. Instead, we determined that the G6PD-PPP metabolic pathway regulates acetyl-CoA/H3K9ac/Gzmb pathway to activate tumor-specific CTLs. Tumor cells therefore may use H3K9me3 deposition at the *G6pd* promoter to downregulate G6PD expression to impair PPP to divert glucose metabolic flux to glycolysis, resulting in impaired PPP and CTL exhaustion. Accordingly, pharmacological activation of G6PD reverses CTL exhaustion to increase tumor-specific CTL lytic function in vitro and to suppress tumor growth in vivo. Translationally, we determined that granzyme B expression level, not CTL tumor-infiltration level, correlates with the survival of patients with epithelioid mesothelioma. Our data indicate that targeting G6PD epigenetic downregulation is potentially an effective approach to reinvigorate tumor-induced exhaustion

of tumor-specific CTLs to suppress tumor growth in human mesothelioma cancer immunotherapy.

Author affiliations

- ¹School of Life Sciences, Tianjin University, Tianjin, China
²Department of Biochemistry and Molecular Biology, Medical College of Georgia, Augusta, GA, USA
³Georgia Cancer Center, Medical College of Georgia, Augusta, GA, USA
⁴Charlie Norwood VA Medical Center, Augusta, GA, USA
⁵Division of Thoracic Surgery, Department of Surgery, Massachusetts General Hospital, Harvard Medical School, Boston, MA, USA
⁶Department of Chemistry and Biochemistry, University of North Carolina at Greensboro, Greensboro, NC, USA
⁷Mycosynthetix Inc, Hillsborough, NC, USA
⁸Ionic Pharmaceuticals, Brookline, MA, USA
⁹Department of Biomedical Engineering, Boston University, Boston, MA, USA

Acknowledgements We thank Dr Jeanene Pihkala at Georgia Cancer Center Flow Cytometry Core Facility for assistance in flow cytometry analysis.

Contributors CL, YLC, NHO, CJP, AHC, MWG, HS, H-FD, and KL designed the study and wrote or reviewed the manuscript. CL, DY, and JDK, performed experiments, collected data, and analyzed data. HS performed bioinformatics analysis and data analysis. CL acts as guarantor.

Funding This work was supported by the National Cancer Institute (grant numbers R01 CA227433, to MWG, YLC, NHO, and KL; R01CA133085, to KL; P01 CA125066, to NHO; R01CA190429 and R01CA236890, to H-FD; and F30CA236436, to JDK) and US Department of Veterans Affairs (award number CX001364, to KL).

Competing interests None declared.

Patient consent for publication Not applicable.

Ethics approval This study does not involve human participants.

Provenance and peer review Not commissioned; externally peer reviewed.

Data availability statement Data sharing is not applicable as no datasets were generated and/or analyzed for this study.

Supplemental material This content has been supplied by the author(s). It has not been vetted by BMJ Publishing Group Limited (BMJ) and may not have been peer-reviewed. Any opinions or recommendations discussed are solely those of the author(s) and are not endorsed by BMJ. BMJ disclaims all liability and responsibility arising from any reliance placed on the content. Where the content includes any translated material, BMJ does not warrant the accuracy and reliability of the translations (including but not limited to local regulations, clinical guidelines, terminology, drug names and drug dosages), and is not responsible for any error and/or omissions arising from translation and adaptation or otherwise.

Open access This is an open access article distributed in accordance with the Creative Commons Attribution Non Commercial (CC BY-NC 4.0) license, which permits others to distribute, remix, adapt, build upon this work non-commercially, and license their derivative works on different terms, provided the original work is properly cited, appropriate credit is given, any changes made indicated, and the use is non-commercial. See <http://creativecommons.org/licenses/by-nc/4.0/>.

ORCID iD

Kebin Liu <http://orcid.org/0000-0003-1965-7240>

REFERENCES

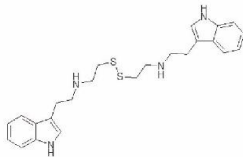
- Hotta K, Fujimoto N. Current evidence and future perspectives of immune-checkpoint inhibitors in unresectable malignant pleural mesothelioma. *J Immunother Cancer* 2020;8.
- Gray SG. Emerging avenues in immunotherapy for the management of malignant pleural mesothelioma. *BMC Pulm Med* 2021;21:148.
- Alley EW, Lopez J, Santoro A, et al. Clinical safety and activity of pembrolizumab in patients with malignant pleural mesothelioma (KEYNOTE-028): preliminary results from a non-randomised, open-label, phase 1B trial. *Lancet Oncol* 2017;18:623–30.
- Quispel-Janssen J, van der Noort V, de Vries JF, et al. Programmed death 1 blockade with nivolumab in patients with recurrent malignant pleural mesothelioma. *J Thorac Oncol* 2018;13:1569–76.
- Yap TA, Nakagawa K, Fujimoto N, et al. Efficacy and safety of pembrolizumab in patients with advanced mesothelioma in the open-label, single-arm, phase 2 KEYNOTE-158 study. *Lancet Respir Med* 2021;9:613–21.
- Bronte G, Delmonte A, Burgio MA, et al. Impressive clinical response to anti-PD-1 therapy in epithelioid mesothelioma with high clonal PD-L1 expression and EML4-ALK rearrangement. *Lung Cancer* 2020;142:47–50.
- Marcq E, Siozopoulou V, De Waele J, et al. Prognostic and predictive aspects of the tumor immune microenvironment and immune checkpoints in malignant pleural mesothelioma. *Oncoimmunology* 2017;6:e1261241.
- Patil NS, Righi L, Koeppen H, et al. Molecular and histopathological characterization of the tumor immune microenvironment in advanced stage of malignant pleural mesothelioma. *J Thorac Oncol* 2018;13:124–33.
- Wadowski B, De Rienzo A, Bueno R. The molecular basis of malignant pleural mesothelioma. *Thorac Surg Clin* 2020;30:383–93.
- Mankor JM, Disselhorst MJ, Poncin M, et al. Efficacy of nivolumab and ipilimumab in patients with malignant pleural mesothelioma is related to a subtype of effector memory cytotoxic T cells: translational evidence from two clinical trials. *EBioMedicine* 2020;62:103040.
- Hurkmans DP, Basak EA, Schepers N, et al. Granzyme B is correlated with clinical outcome after PD-1 blockade in patients with stage IV non-small-cell lung cancer. *J Immunother Cancer* 2020;8:e000586.
- Peng M, Yin N, Chhangawala S, et al. Aerobic glycolysis promotes T helper 1 cell differentiation through an epigenetic mechanism. *Science* 2016;354:481–4.
- Chang C-H, Curtis JD, Maggi LB, et al. Posttranscriptional control of T cell effector function by aerobic glycolysis. *Cell* 2013;153:1239–51.
- Macintyre AN, Gerriets VA, Nichols AG, et al. The glucose transporter GLUT1 is selectively essential for CD4 T cell activation and effector function. *Cell Metab* 2014;20:61–72.
- Cascone T, McKenzie JA, Mbofung RM, et al. Increased tumor glycolysis characterizes immune resistance to adoptive T cell therapy. *Cell Metab* 2018;27:977–87.
- Leone RD, Zhao L, Englert JM, et al. Glutamine blockade induces divergent metabolic programs to overcome tumor immune evasion. *Science* 2019;366:1013–21.
- Ghergurovich JM, Esposito M, Chen Z, et al. Glucose-6-phosphate dehydrogenase is not essential for K-ras-driven tumor growth or metastasis. *Cancer Res* 2020;80:3820–9.
- Nakamura M, Nagase K, Yoshimitsu M, et al. Glucose-6-phosphate dehydrogenase correlates with tumor immune activity and programmed death ligand-1 expression in Merkel cell carcinoma. *J Immunother Cancer* 2020;8.
- Kumar A, Pyram K, Yarosz EL, et al. Enhanced oxidative phosphorylation in NKT cells is essential for their survival and function. *Proc Natl Acad Sci U S A* 2019;116:7439–48.
- Zimmerman M, Hu X, Liu K. Experimental metastasis and CTL adoptive transfer immunotherapy mouse model. *J Vis Exp* 2010;2010:45.
- Hwang S, Mruk K, Rahighi S, et al. Correcting glucose-6-phosphate dehydrogenase deficiency with a small-molecule activator. *Nat Commun* 2018;9:4045.
- Lu C, Klement JD, Smith AD, et al. P50 suppresses cytotoxic T lymphocyte effector function to regulate tumor immune escape and response to immunotherapy. *J Immunother Cancer* 2020;8.
- Tan Z, Chiu MS, Yan CW, et al. Eliminating mesothelioma by AAV-vectored, PD1-based vaccination in the tumor microenvironment. *Mol Ther Oncolytics* 2021;20:373–86.
- Ryan MH, Bristol JA, McDuffie E, et al. Regression of extensive pulmonary metastases in mice by adoptive transfer of antigen-specific CD8(+) CTL reactive against tumor cells expressing a naturally occurring rejection epitope. *J Immunol* 2001;167:4286–92.
- Frauwirth KA, Thompson CB. Regulation of T lymphocyte metabolism. *J Immunol* 2004;172:4661–5.
- Vroman H, Balzaretto G, Belderbos RA, et al. T cell receptor repertoire characteristics both before and following immunotherapy correlate with clinical response in mesothelioma. *J Immunother Cancer* 2020;8:e000251.
- Sen DR, Kaminski J, Barnitz RA, et al. The epigenetic landscape of T cell exhaustion. *Science* 2016;354:1165–9.
- Ding J, Li T, Wang X, et al. The histone H3 methyltransferase G9A epigenetically activates the serine-glycine synthesis pathway to sustain cancer cell survival and proliferation. *Cell Metab* 2013;18:896–907.
- Pace L, Goudot C, Zueva E, et al. The epigenetic control of stemness in CD8+ T cell fate commitment. *Science* 2018;359:177–86.
- Lu C, Yang D, Klement JD, et al. SUV39H1 represses the expression of cytotoxic T-lymphocyte effector genes to promote colon tumor immune evasion. *Cancer Immunol Res* 2019;7:414–27.



- 31 Paschall AV, Yang D, Lu C, *et al.* H3K9 trimethylation silences Fas expression to confer colon carcinoma immune escape and 5-fluorouracil chemoresistance. *J Immunol* 2015;195:1868–82.
- 32 Nicetto D, Donahue G, Jain T, *et al.* H3K9me3-heterochromatin loss at protein-coding genes enables developmental lineage specification. *Science* 2019;363:294–7.
- 33 To T-L, Cuadros AM, Shah H, *et al.* A compendium of genetic modifiers of mitochondrial dysfunction reveals intra-organelle buffering. *Cell* 2019;179:e17:1222–38.
- 34 Amitrano AM, Berry BJ, Lim K, *et al.* Optical Control of CD8⁺ T Cell Metabolism and Effector Functions. *Front Immunol* 2021;12:666231.
- 35 Martínez-Reyes I, Diebold LP, Kong H, *et al.* Tca cycle and mitochondrial membrane potential are necessary for diverse biological functions. *Mol Cell* 2016;61:199–209.
- 36 Wahlbuhl E, Liehr T, Rincic M, *et al.* Cytogenomic characterization of three murine malignant mesothelioma tumor cell lines. *Mol Cytogenet* 2020;13:43.
- 37 Ma J, Zheng B, Goswami S, *et al.* PD1^{hi} CD8⁺ T cells correlate with exhausted signature and poor clinical outcome in hepatocellular carcinoma. *J Immunother Cancer* 2019;7:331.
- 38 Gueguen P, Metoikidou C, Dupic T, *et al.* Contribution of resident and circulating precursors to tumor-infiltrating CD8⁺ T cell populations in lung cancer. *Sci Immunol* 2021;6. doi:10.1126/sciimmunol.abd5778. [Epub ahead of print: 29 01 2021].
- 39 Xu K, Yin N, Peng M, *et al.* Glycolysis fuels phosphoinositide 3-kinase signaling to bolster T cell immunity. *Science* 2021;371:405–10.
- 40 Zhu J, Petit P-F, Van den Eynde BJ. Apoptosis of tumor-infiltrating T lymphocytes: a new immune checkpoint mechanism. *Cancer Immunol Immunother* 2019;68:835–47.
- 41 Siegel RM, Frederiksen JK, Zacharias DA, *et al.* Fas preassociation required for apoptosis signaling and dominant inhibition by pathogenic mutations. *Science* 2000;288:2354–7.
- 42 Yost KE, Satpathy AT, Wells DK, *et al.* Clonal replacement of tumor-specific T cells following PD-1 blockade. *Nat Med* 2019;25:1251–9.
- 43 Miller BC, Sen DR, Al Abosy R, *et al.* Subsets of exhausted CD8⁺ T cells differentially mediate tumor control and respond to checkpoint blockade. *Nat Immunol* 2019;20:326–36.
- 44 Inaguma S, Lasota J, Czapiewski P, *et al.* CD70 expression correlates with a worse prognosis in malignant pleural mesothelioma patients via immune evasion and enhanced invasiveness. *J Pathol* 2020;250:205–16.
- 45 Losi L, Bertolini F, Guaitoli G, *et al.* Role of evaluating tumor-infiltrating lymphocytes, programmed death-1 ligand 1 and mismatch repair proteins expression in malignant mesothelioma. *Int J Oncol* 2019;55:1157–64.
- 46 Pasello G, Zago G, Lunardi F, *et al.* Malignant pleural mesothelioma immune microenvironment and checkpoint expression: correlation with clinical-pathological features and intratumor heterogeneity over time. *Ann Oncol* 2018;29:1258–65.
- 47 Marcq E, Pauwels P, van Meerbeeck JP, *et al.* Targeting immune checkpoints: new opportunity for mesothelioma treatment? *Cancer Treat Rev* 2015;41:914–24.
- 48 Thapa B, Salcedo A, Lin X, *et al.* The immune microenvironment, genome-wide copy number aberrations, and survival in mesothelioma. *J Thorac Oncol* 2017;12:850–9.
- 49 Zhang M, Luo J-L, Sun Q, *et al.* Clonal architecture in mesothelioma is prognostic and shapes the tumour microenvironment. *Nat Commun* 2021;12.
- 50 Noordam L, Kaijen MEH, Bezemer K, *et al.* Low-dose cyclophosphamide depletes circulating naïve and activated regulatory T cells in malignant pleural mesothelioma patients synergistically treated with dendritic cell-based immunotherapy. *Oncoimmunology* 2018;7:e1474318.

Supplemental Data

MaxPeak: 100.00%
Ret_Time: 0.969 min



Mol Wt 438.66
Exact Mass 438

#	Time	Area%
1	0.969	100.00

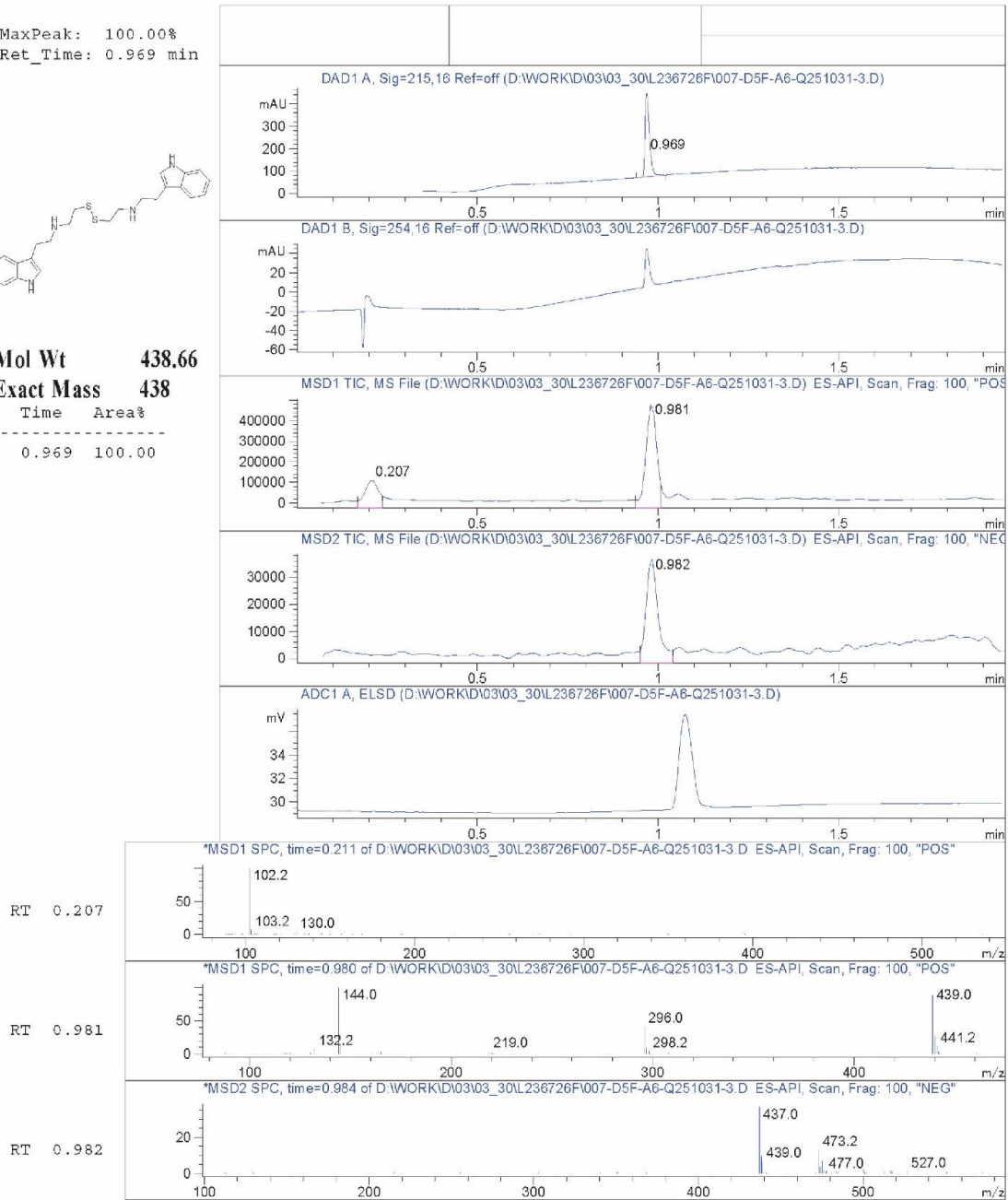


Figure S1. Quality control analysis of chemically synthesized AG1.

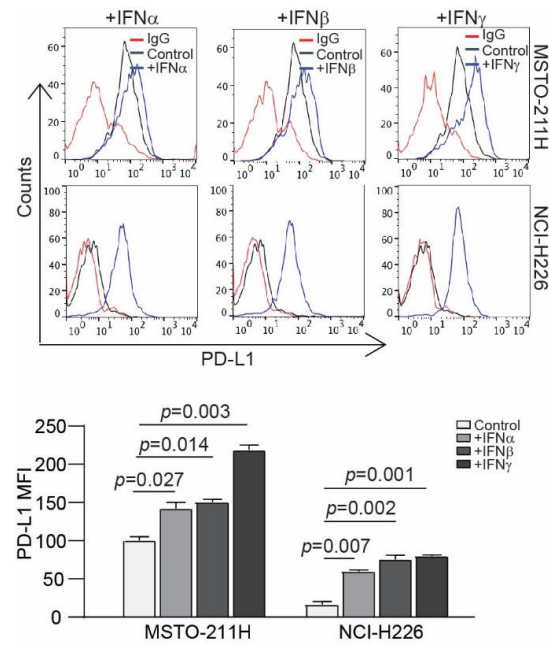


Figure S2. Human mesothelioma cells express high level of PD-L1. MSTO-211H and NCI-H226 cells were treated by hIFN α , hIFN β and hIFN γ overnight and analyzed for PD-L1 expression by flow cytometry. The MFI of PD-L1 were quantified and presented at the bottom panel.

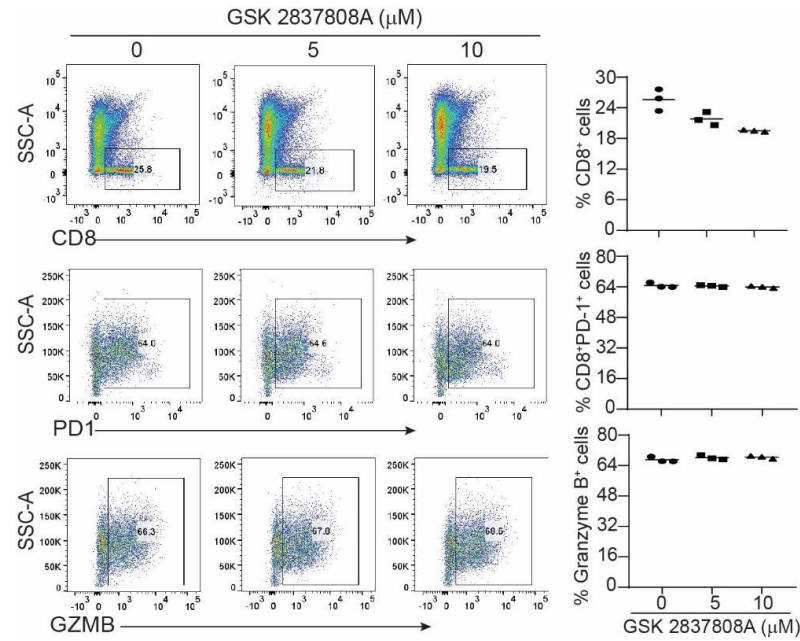


Figure S3. Inhibition of LDHA has no significant effect on CTLs effector and exhaustion marker expression. 2/20 CTLs were co-cultured with AB1 cells for 24h, treated by GSK 2837808A at indicated concentrations and analyzed by flow cytometry for CD8, PD-1, and Gzmb. Representative dot plots are shown at left panel. Percentage of positive cells are shown at right panel.

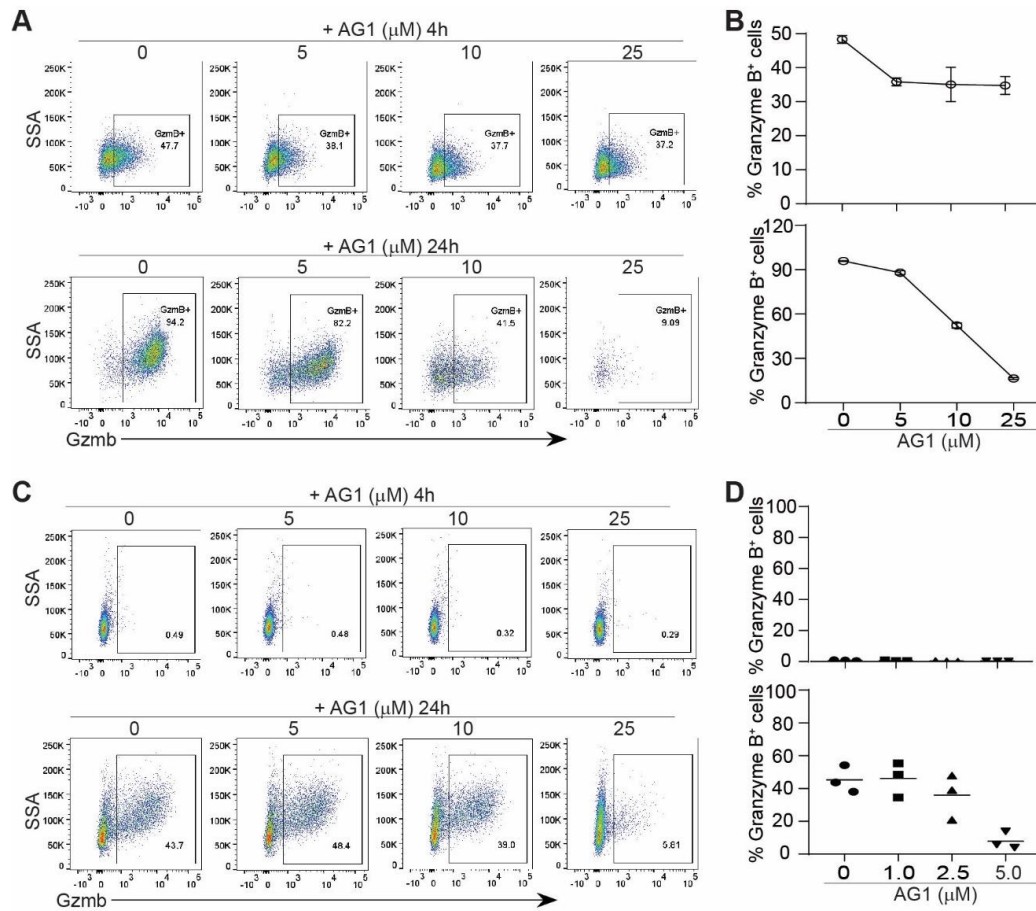


Figure S4. G6PD suppresses *Gzmb* expression in activated antigen-specific CTLs and primary CD8⁺ T cells. **A.** 2/20 CTLs were stimulated by AH1 peptide for 4h and 24h, treated by AG1 at indicated concentrations and analyzed by flow cytometry for CD8 and *Gzmb*. **B.** Percentage of *Gzmb* positive cells were quantified and presented. **C.** Primary CD8⁺ T cells purified from mouse spleens were stimulated by anti-CD3/28 antibodies for 4h and 24h, treated by AG1 at indicated concentrations and analyzed by flow cytometry for CD8 and *Gzmb*. **D.** Percentage of *Gzmb* positive cells were quantified and presented.

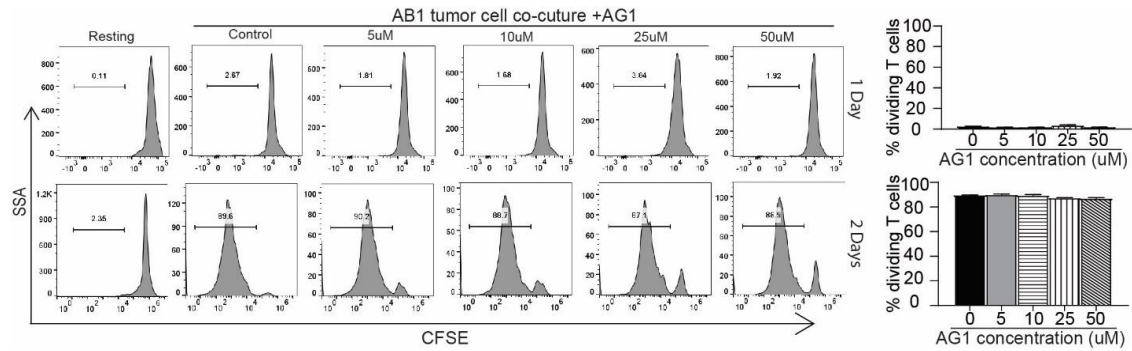


Figure S5. G6PD does not regulate tumor-specific CTLs proliferation. CFSE labeled-2/20 CTLs were cultured with AB1 cells for 24h and 48h, treated with AG1 at indicated concentrations and analyzed by flow cytometry. Percentage of dividing T cells were quantified and presented at the right.

Table S1. Reagents

Reagent	Source	Cat #
Antibodies		
PerCP-CD8(53-6.7)	Biologend	100732; RRID: AB_893423
Pacific Blue-GzmB (GB11)	Biologend	515408;RRID: AB_2562196
APC-gp70	MBL	TS-M521-2
PE/Cy7-CD45(104)	Biologend	109830; RRID:AB_1186093
Pacific Blue-Hamster IgG2, kappa (B81-3)	BD Pharmingen	560317
APC-Rat IgG2a, kappa (RTK2758)	Biologend	400512
PE-Rat IgG2b, kappa (RTK4530)	Biologend	400636
Ki67	Novus	NB500-170
Acetyl-Histone H3 (Lys9) (C5B11)	Cell Signaling Technology	9649
Anti-Histone H3 (tri methyl K9) antibody	Abcam	8898
Normal Rabbit IgG	Cell Signaling Technology	2729P
FITC-CD8	Biologend	100706
PE-PD-1 (29F.1A12)	Biologend	135206; RRID:AB_1877231
APC-PD-L1(10F.9G2)	Biologend	124312; RRID:AB_1061271
InVivoPlus Anti-mCD3e (145-2C11)	BioXcell	BP0001-1 RRID:AB_1107634
InVivoPlus Anti-mCD28 (37.51)	BioXcell	BE0015-1; RRID:AB_1107624
Chemicals, Peptides, Recombinant Proteins		
Verticillin A	In house	Figuroa et al., 2012
AG1	Customer synthesis, LeadGen Labs,	Hwang et al., 2018
AH1 peptide (SPSYVYHGF)	Genscript	N/A
Recombinant human IFN α (carrier free)	Biologend	592704
Recombinant human IFN β (carrier free)	Peprotech	300-028C-20UG
Recombinant human IFN γ (carrier free)	R&D	285-IF/CF
Recombinant mouse IFN α (carrier free)	R&D	12100-1
Recombinant mouse IFN β (carrier free)	Biologend	576306
Recombinant mouse IFN γ (carrier free)	Biologend	575306
Propidium iodide	EMD Millipore	537059
Commercial Assay Kits		
Acetyl-Coenzyme A Assay Kit	Sigma	100706
Lactate Assay Kit II	Sigma	MAK065
CellTrace™ CFSE Cell Proliferation Kit	Life Technologies	C34554

SimpleChIP® Plus Enzymatic Chromatin IP Kit (Agarose Beads)	Cell Signaling Transduction	9004
Oligonucleotide		
mG6pdx-F	TTGCCCCCACAGTCTATGAAG	
mG6pdx-B	TTCTCCACGATGATGCGGTTCC	
mG6pdx ChIP1-F	TGAAACCTTCTTCTGACTCCCTT	
mG6pdx ChIP1-B	CACACCCCATTACAATCCTTTA	
mG6pdx ChIP2-F	CTTGCGGCAGAACAAACTGG	
mG6pdx ChIP2-B	TCTCCAAAGACAGGGCTCCATC	
mG6pdx ChIP3-F	ACAGAGTGTGATGCCGTAACCA	
mG6pdx ChIP3-B	ACCTCCAAAGTTGCCTTCGC	
mGzmb ChIP1-F	TGTTGCTGTGCTGGTCATTGTG	
mGzmb ChIP1-B	CTCAGGGTGCTGTGCCAAAG	
mGzmb ChIP2-F	ACCAGGCTCTTCCCATCCTTAG	
mGzmb ChIP2-B	CGTGGCAAACCCATTCTTATG	
mGzmb ChIP3-F	GTGTTTATGACCCCGAGTAGA	
mGzmb ChIP3-B	GAGCCCTGTGAAGCACTGAGTT	